The Astrophysical Journal, 883:135 (9pp), 2019 October 1 https://doi.org/10.3847/1538-4357/ab3a51


# Constraints on Gamma-Ray and Neutrino Emission from NGC 1068 with the MAGIC Telescopes

V. A. Acciari[1], S. Ansoldi[2,3,4,5,6], L. A. Antonelli[7], A. Arbet Engels[8], D. Baack[9], A. Babić[10,11,12,13,14], B. Banerjee[15], U. Barres de Almeida[16,44], J. A. Barrio[17], J. Becerra González[1], W. Bednarek[18], L. Bellizzi[19], E. Bernardini[20,21,22], A. Berti[2,45], J. Besenrieder[16], W. Bhattacharyya[21], C. Bigongiari[7], A. Biland[8], O. Blanch[23], G. Bonnoli[19], Ž. Bošnjak[24,25,26,27,28], G. Busetto[20], R. Carosi[29], G. Ceribella[16], Y. Chai[16], A. Chilingaryan[30], S. Cikota[24,25,26,27,28], S. M. Colak[23], U. Colin[16], E. Colombo[1], J. L. Contreras[17], J. Cortina[23], S. Covino[7], V. D'Elia[7], P. Da Vela[19], F. Dazzi[7], A. De Angelis[20], B. De Lotto[2], M. Delfino[23,46], J. Delgado[23], D. Depaoli[31], F. Di Pierro[20], L. Di Venere[31], E. Do Souto Espiñeira[23], D. Dominis Prester[10,11,12,13,14], A. Donini[2], D. Dorner[32], M. Doro[20], D. Elsaesser[9], V. Fallah Ramazani[33,34], A. Fattorini[9], G. Ferrara[7], D. Fidalgo[17], L. Foffano[20], M. V. Fonseca[17], L. Font[35], C. Fruck[16], S. Fukami[3,4,5,6], R. J. García López[1], M. Garczarczyk[21], S. Gasparyan[30], M. Gaug[35], N. Giglietto[31], F. Giordano[31], N. Godinović[10,11,12,13,14], D. Green[16], D. Guberman[23], D. Hadasch[3,4,5,6], A. Hahn[16], J. Herrera[1], J. Hoang[17], D. Hrupec[10,11,12,13,14], M. Hütten[16], T. Inada[3,4,5,6], S. Inoue[3,4,5,6], K. Ishio[16], Y. Iwamura[3,4,5,6], L. Jouvin[23], D. Kerszberg[23], H. Kubo[3,4,5,6], J. Kushida[3,4,5,6], A. Lamastra[7], D. Lelas[10,11,12,13,14], F. Leone[7], E. Lindfors[33,34], S. Lombardi[7], F. Longo[2,45], M. López[17], R. López-Coto[36], A. López-Oramas[1], S. Loporchio[31], B. Machado de Oliveira Fraga[37], C. Maggio[35], P. Majumdar[15], M. Makariev[38], M. Mallamaci[20], G. Maneva[38], M. Manganaro[1], K. Mannheim[32], L. Maraschi[7], M. Mariotti[20], M. Martínez[23], D. Mazin[3,4,5,6,16], S. Mićanović[24,25,26,27,28], D. Miceli[2], M. Minev[38], J. M. Miranda[19], R. Mirzoyan[16], E. Molina[39], A. Moralejo[23], D. Morcuende[36], V. Moreno[35], E. Moretti[23], P. Munar-Adrover[35], V. Neustroev[33,34], C. Nigro[21], K. Nilsson[33,34], D. Ninci[23], K. Nishijima[3,4,5,6], K. Noda[3,4,5,6], L. Nogués[23], S. Nozaki[3,4,5,6], S. Paiano[20], J. Palacio[23], M. Palatiello[2], D. Paneque[16], R. Paoletti[19], J. M. Paredes[40], P. Peñil[17], M. Peresano[2], M. Persic[2,47], P. G. Prada Moroni[29], E. Prandini[20], I. Puljak[10,11,12,13,14], W. Rhode[9], M. Ribó[40], J. Rico[23], C. Righi[7], A. Rugliancich[19], L. Saha[17], N. Sahakyan[30], T. Saito[3,4,5,6], S. Sakurai[3,4,5,6], K. Satalecka[21], K. Schmidt[9], T. Schweizer[16], J. Sitarek[18], I. Šnidarić[10,11,12,13,14], D. Sobczynska[18], A. Somero[1], A. Stamerra[7], D. Strom[16], M. Strzys[16], Y. Suda[16], T. Surić[10,11,12,13,14], M. Takahashi[3,4,5,6], F. Tavecchio[7], P. Temnikov[38], T. Terzić[10,11,12,13,14], M. Teshima[3,4,5,6,16], N. Torres-Albà[40], L. Tosti[31], V. Vagelli[31], J. van Scherpenberg[16], G. Vanzo[1], M. Vazquez Acosta[1], C. F. Vigorito[31], V. Vitale[31], I. Vovk[16], M. Will[16], D. Zarić[10,11,12,13,14]

MAGIC Collaboration,

F. Fiore[41], C. Feruglio[41], and Y. Rephaeli[42,43]

[1] Inst. de Astrofísica de Canarias, E-38200 La Laguna, and Universidad de La Laguna, Dpto. Astrofísica, E-38206 La Laguna, Tenerife, Spain
[2] Università di Udine, and INFN Trieste, I-33100 Udine, Italy
[3] Japanese MAGIC Consortium, ICRR, The University of Tokyo, 277-8582 Chiba, Japan
[4] Japanese MAGIC Consortium, Department of Physics, Kyoto University, 606-8502 Kyoto, Japan
[5] Japanese MAGIC Consortium, Tokai University, 259-1292 Kanagawa, Japan
[6] Japanese MAGIC Consortium, RIKEN, 351-0198 Saitama, Japan
[7] National Institute for Astrophysics (INAF), I-00136 Rome, Italy; alessandra.lamastra@inaf.it, saverio.lombardi@inaf.it, antonio.stamerra@inaf.it
[8] ETH Zurich, CH-8093 Zurich, Switzerland
[9] Technische Universität Dortmund, D-44221 Dortmund, Germany
[10] Croatian MAGIC Consortium, University of Rijeka, 51000 Rijeka, Croatia
[11] Croatian MAGIC Consortium, University of Split—FESB, 21000 Split, Croatia
[12] Croatian MAGIC Consortium, University of Zagreb—FER, 10000 Zagreb, Croatia
[13] Croatian MAGIC Consortium, University of Osijek, 31000 Osijek, Croatia
[14] Croatian MAGIC Consortium, Rudjer Boskovic Institute, 10000 Zagreb, Croatia
[15] Saha Institute of Nuclear Physics, HBNI, 1/AF Bidhannagar, Salt Lake, Sector-1, Kolkata 700064, India
[16] Max-Planck-Institut für Physik, D-80805 München, Germany
[17] Unidad de Partículas y Cosmología (UPARCOS), Universidad Complutense, E-28040 Madrid, Spain
[18] University of Łódź, Department of Astrophysics, PL-90236 Łódź, Poland
[19] Università di Siena and INFN Pisa, I-53100 Siena, Italy
[20] Università di Padova and INFN, I-35131 Padova, Italy
[21] Deutsches Elektronen-Synchrotron (DESY), D-15738 Zeuthen, Germany
[22] Humboldt University of Berlin, Institut für Physik D-12489 Berlin Germany
[23] Institut de Física d'Altes Energies (IFAE), The Barcelona Institute of Science and Technology (BIST), E-08193 Bellaterra (Barcelona), Spain
[24] Croatian Consortium, University of Rijeka, Department of Physics, 51000 Rijeka, Croatia
[25] Croatian Consortium, University of Split—FESB, 21000 Split, Croatia
[26] Croatian Consortium, University of Zagreb—FER, 10000 Zagreb, Croatia
[27] Croatian Consortium, University of Osijek, 31000 Osijek, Croatia
[28] Croatian Consortium, Rudjer Boskovic Institute, 10000 Zagreb, Croatia
[29] Università di Pisa, and INFN Pisa, I-56126 Pisa, Italy
[30] ICRANet-Armenia at NAS RA, 0019 Yerevan, Armenia
[31] Istituto Nazionale Fisica Nucleare (INFN), I-00044 Frascati (Roma), Italy
[32] Universität Würzburg, D-97074 Würzburg, Germany
[33] Finnish MAGIC Consortium, Tuorla Observatory and Finnish Centre of Astronomy with ESO (FINCA), University of Turku, Vaisalantie 20, FI-21500 Piikkiö, Finland

[34] Finnish MAGIC Consortium, Astronomy Division, University of Oulu, FI-90014 University of Oulu, Finland
[35] Departament de Física, and CERES-IEEC, Universitat Autónoma de Barcelona, E-08193 Bellaterra, Spain
[36] IPARCOS Institute and EMFTEL Department, Universidad Complutense de Madrid, E-28040 Madrid, Spain
[37] Centro Brasileiro de Pesquisas Físicas (CBPF), 22290-180 URCA, Rio de Janeiro (RJ), Brasil
[38] Inst. for Nucl. Research and Nucl. Energy, Bulgarian Academy of Sciences, BG-1784 Sofia, Bulgaria
[39] Universitat de Barcelona, ICCUB, IEEC-UB, E-08028 Barcelona, Spain
[40] Universitat de Barcelona, ICC, IEEC-UB, E-08028 Barcelona, Spain
[41] INAF Osservatorio Astronomico di Trieste, via Tiepolo 11, I-34143 Trieste, Italy
[42] School of Physics and Astronomy, Tel Aviv University, Tel Aviv, Israel
[43] CASS, University of California, San Diego, La Jolla, CA, USA
*Received 2019 June 26; revised 2019 July 26; accepted 2019 August 6; published 2019 September 27*

## Abstract

Starburst galaxies and star-forming active galactic nuclei are among the candidate sources thought to contribute appreciably to the extragalactic gamma-ray and neutrino backgrounds. NGC 1068 is the brightest of the star-forming galaxies found to emit gamma-rays from 0.1 to 50 GeV. Precise measurements of the high-energy spectrum are crucial to study the particle accelerators and probe the dominant emission mechanisms. We have carried out 125 hr of observations of NGC 1068 with the MAGIC telescopes in order to search for gamma-ray emission in the very-high-energy band. We did not detect significant gamma-ray emission, and set upper limits at the 95% confidence level to the gamma-ray flux above 200 GeV $f < 5.1 \times 10^{-13}\,\mathrm{cm}^{-2}\,\mathrm{s}^{-1}$. This limit improves previous constraints by about an order of magnitude and allows us to put tight constraints on the theoretical models for the gamma-ray emission. By combining the MAGIC observations with the *Fermi*-LAT spectrum we limit the parameter space (spectral slope, maximum energy) of the cosmic ray protons predicted by hadronuclear models for the gamma-ray emission, while we find that a model postulating leptonic emission from a semi-relativistic jet is fully consistent with the limits. We provide predictions for IceCube detection of the neutrino signal foreseen in the hadronic scenario. We predict a maximal IceCube neutrino event rate of $0.07\,\mathrm{yr}^{-1}$.

*Unified Astronomy Thesaurus concepts:* Active galaxies (17); Starburst galaxies (1570); Gamma-ray sources (633)

## 1. Introduction

The cumulative gamma-ray and neutrino emission from star-forming galaxies, including starbursts and star-forming active galactic nuclei (AGNs), has been proposed to contribute to the extragalactic gamma-ray and neutrino backgrounds (e.g., Tamborra et al. 2014; Wang & Loeb 2016; Lamastra et al. 2017; Liu et al. 2018). However, their exact contributions to the diffuse fluxes measured by the Large Area Telescope (LAT) on board the *Fermi Gamma-ray Space Telescope (Fermi)* (Ackermann et al. 2015) and IceCube (Aartsen et al. 2015) still have to be established. Due to observational uncertainties in the measured spectra, the exact emission mechanisms and their parameters remain unknown.

The gamma-ray emission in star-forming galaxies is expected to be predominantly produced from cosmic ray (CR) interactions with gas. In these astrophysical environments CRs accelerated by supernova (SN) remnants interact with the interstellar medium (ISM) and produce neutral and charged pions which in turn decay into high-energy gamma-rays and neutrinos (e.g., Persic et al. 2008; Rephaeli et al. 2010; Yoast-Hull et al. 2014; Eichmann & Becker Tjus 2016). Starburst galaxies exhibit higher star formation rate (SFR $\simeq$ 10–100 $M_\odot\,\mathrm{yr}^{-1}$) compared to quiescently star-forming galaxies such as our Galaxy (SFR $\simeq$ 1–5 $M_\odot\,\mathrm{yr}^{-1}$, Smith et al. 1978; Murray & Rahman 2010). Given the expected CR energy input from SN explosions and the dense gas present in starburst nuclei, starburst galaxies are expected to be more powerful gamma-ray emitters than normal star-forming galaxies. The starburst mode of star formation is likely triggered by galaxy interactions (major and minor mergers), as suggested by observational evidence and theoretical arguments (e.g., Hernquist 1989; Sanders & Mirabel 1996; Somerville et al. 2001; Lamastra et al. 2013a). Consequently, galaxy interactions also enhance the accretion of gas into the central supermassive black hole and the ensuing AGN activity. The latter is also associated with galaxies undergoing secular evolution. Studies on the star-forming properties of AGN host galaxies indicate that the level of star formation in AGN hosts can be either elevated, as in starbursts, or normal, as in quiescently star-forming galaxies, or suppressed, as in passive spheroids (see Lamastra et al. 2013b; Gatti et al. 2015; Rodighiero et al. 2015 and references therein). In active galaxies, non-thermal radiation in the gamma-ray band may also be produced by the interaction of particles (protons and electrons) accelerated in AGN-driven outflows (wind and jet) with the ISM and interstellar radiation fields (e.g., Lenain et al. 2010; Tamborra et al. 2014; Lamastra et al. 2016, 2019). Indeed, weak misaligned radio jets, and wide-angle AGN-driven outflows have been observed in star-forming AGNs detected in the GeV band by *Fermi*-LAT (Gallimore et al. 1996; Elmouttie et al. 1998; García-Burillo et al. 2014; Zschaechner et al. 2016). The AGN contribution to gamma-ray emission is supported by the comparison between the galaxy non-thermal luminosity and the CR luminosity provided by star formation. In starburst galaxies a fraction equal to ~0.3–0.6 of CR energy input is estimated to be converted into radiation in the gamma-ray band, while calorimetric fractions close to one, and even larger, have been observed in star-forming AGNs (Ackermann et al. 2012; Wang & Fields 2018).

The gamma-ray spectra of nearby starbursts and AGNs have been measured in the high-energy (HE, 0.1–100 GeV) band by *Fermi*-LAT (Ackermann et al. 2012; Hayashida et al. 2013; Tang et al. 2014; Acero et al. 2015; Lamastra et al. 2016;

[44] Present address: Centro Brasileiro de Pesquisas Físicas (CBPF), 22290-180 URCA, Rio de Janeiro (RJ), Brasil.
[45] Present address: Dipartimento di Fisica, Università di Trieste, I-34127 Trieste, Italy.
[46] Present address: Port d'Informació Científica (PIC) E-08193 Bellaterra (Barcelona), Spain.
[47] Present address: INAF-Trieste and Dept. of Physics & Astronomy, University Of Bologna, Italy.

Peng et al. 2016; Ajello et al. 2017; Wojaczyński & Niedźwiecki 2017). The starburst galaxies NGC 253 and M82 have also been detected in the very-high-energy (VHE, 0.1–100 TeV) band with Imaging Atmospheric Cherenkov Telescopes (IACTs; Acciari et al. 2009; Acero et al. 2009). These two measurements are compatible and indicate that the gamma-ray spectra can be described by a single power law with spectral index $p \sim 2.2$ up to TeV energies.

In this paper we present observations in the VHE band of the Seyfert galaxy NGC 1068 with the Major Atmospheric Gamma-ray Imaging Cherenkov (MAGIC) telescopes. NGC 1068, located at a distance of $D = 14.4$ Mpc, was detected in the gamma-ray band by *Fermi*-LAT (Ackermann et al. 2012; Ajello et al. 2017). The latest spectral analysis based on 8 yr of survey data in the 50 MeV–1 TeV range yields a power-law index of ∼2.4 and a flux integrated between 1 and 100 GeV of $5.8 \times 10^{-13}\,\mathrm{cm^{-2}\,s^{-1}}$ (The Fermi-LAT Collaboration 2019). Observations at lower frequencies have revealed the presence of both starburst and AGN activities. Interferometric observations in the millimeter band have identified a ∼2 kpc starburst ring that surrounds a central molecular disk of 350 pc × 200 pc size in which a sizeable fraction of the gas content is involved in a massive AGN-driven wind (Krips et al. 2011; García-Burillo et al. 2014). AGN-driven jets on scales from hundreds of parsecs to kiloparsecs have been observed in the radio band (Gallimore et al. 1996).

Given the very different particle acceleration sites in an active galaxy, the exact origin of the measured high-energy gamma-ray emission in NGC 1068 is still undetermined.

The gamma-ray spectra predicted by the starburst, AGN jet, and AGN wind models that have been proposed in the literature differ significantly in the VHE band where IACTs are more sensitive than *Fermi*-LAT. The leptonic AGN jet model is characterized by a sharp cutoff at energies ∼100 GeV, while the hadronic starburst and AGN wind models extend to the VHE band, but with different spectral slopes. In order to constrain the competing models, we conducted deep observations (125 hr) of NGC 1068 with the MAGIC telescopes. A detection or an upper limit on the VHE cutoff of the gamma-ray spectrum may provide valuable information on the physical properties of the CR accelerator(s), and on the emission mechanism(s). In particular, understanding the leptonic or hadronic nature of the gamma-ray emission, and the estimate of the maximum energy of accelerated particles has important implications for the neutrino signal expected from this source.

The paper is organized as follows. In Section 2 we present the MAGIC observations and data analysis. In Section 3 we show the gamma-ray spectrum of NGC 1068 obtained by combining *Fermi*-LAT and MAGIC observations, and we derive constraints on the theoretical models for the gamma-ray emission. In Section 4 we discuss the implications of the results, including that related to the neutrino signal. Conclusions follow in Section 5.

## 2. MAGIC Observations and Analysis

MAGIC is a stereoscopic system of two 17 m diameter IACTs situated at the Roque de los Muchachos, on the Canary island of La Palma (28.75°N, 17.86°W), at a height of 2200 m above sea level. NGC 1068 observations were carried out from 2016 to 2019 January at zenith angles between 28° and 50°, in wobble mode (Fomin et al. 1994), with a standard wobble offset of 0.°4.

Observations were taken under different night sky background (NSB) conditions. Under dark night conditions, and for zenith angles <30°, MAGIC reaches a trigger energy threshold of ∼50 GeV, and a sensitivity above 220 GeV of 0.67% ± 0.04% of the Crab Nebula flux in 50 hr of observations (Aleksić et al. 2016). The main effect of moonlight is an increase in the analysis energy threshold[48] and in the systematic uncertainties on the flux normalization. In order to limit the degradation of the energy threshold and of the sensitivity below 10% we selected data samples that were recorded with nominal setting and with NSB $< 8 \times \mathrm{NSB_{dark}}$ (∼90% of the whole data sample). After selecting the data with an aerosol transmission measured to be above 85% that of a clear night, the final sample consists of a total of ∼125 hr of effective observation time of good data.

The data have been analyzed using the standard MAGIC Analysis and Reconstruction Software (MARS), according to the prescriptions given in Ahnen et al. (2017). The recorded shower images were calibrated, cleaned, and parameterized according to Hillas (1985) for each telescope individually. The analysis was performed using appropriate Monte Carlo-simulated gamma-ray and background data to reproduce the observational conditions in each NSB data sample. The data reduction (stereo reconstruction, gamma/hadron separation, and estimation of energy and arrival direction of the primary particle) was performed for each sample separately. The energy threshold, which is obtained by taking into account the actual zenith angle distribution of the selected data, ranges from a minimum of about 140 GeV for the lowest NSB data sample to a maximum of about 300 GeV for the highest NSB data sample. Flux upper limits are calculated following Rolke et al. (2005), with a confidence level of 95%, and considering a systematic error on flux estimation of 30% (Aleksić et al. 2016).

## 3. Results

Figure 1 shows the distribution of the square of the difference between the nominal position of the source and the reconstructed direction in camera coordinates for both the gamma-like events and background events. For the total data set (∼125 hr), we find an excess of 243 gamma-like events over 24320 ± 156 background events, which yields a significance of $1.1\sigma$ (Li & Ma 1983).

By excluding data with an energy threshold larger than 200 GeV (∼23 hr), we derive an integral flux upper limit at the 95% confidence level above 200 GeV of $f < 5.1 \times 10^{-13}\,\mathrm{cm^{-2}\,s^{-1}}$. This limit is lower by about an order of magnitude than the previous estimate by Aharonian et al. (2005). The latter was obtained from 4.3 hr of observations with the High Energy Stereoscopic System (H.E.S.S.) and with a slightly larger energy threshold of 210 GeV.

The differential flux upper limits in the VHE band obtained from the full data sample, as well as the energy spectrum measured with *Fermi*-LAT at lower energies (Acero et al. 2015; Lamastra et al. 2016; Ajello et al. 2017), are shown in Figure 2 (see also Table 1). The gamma-ray emission was detected up to ∼30 GeV by *Fermi*-LAT, while at higher

[48] The analysis energy threshold is obtained by fitting the true energy distribution, which is obtained by reweighting the events with a power-law spectrum of index $p = -2$, with a Gaussian function around its energy peak. We adopt $p = -2$ in the spectral analysis of the VHE data because we expect a component of the gamma-ray emission to be harder than that measured in the HE band with *Fermi*-LAT.

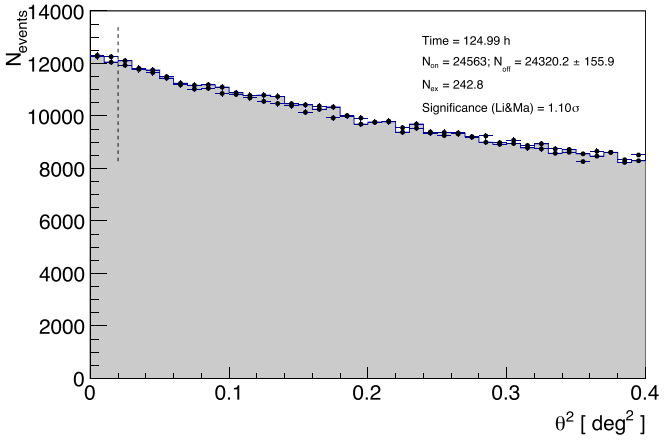


**Figure 1.** Distribution of the square of the difference between the nominal position of the source and the reconstructed direction in camera coordinates for both the gamma-like events (blue crosses) and background events (gray histogram). The vertical dashed line marks the limit of the signal region.

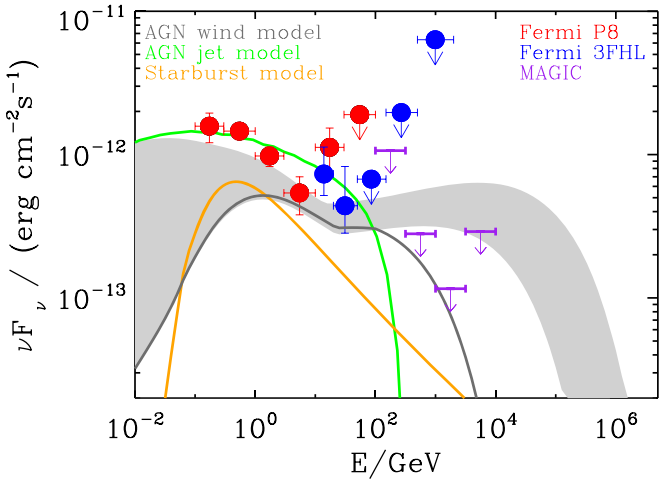


**Figure 2.** Gamma-ray spectrum of NGC 1068 in the HE and VHE bands. The *Fermi*-LAT data points are from Lamastra et al. (2016; P8), and from Ajello et al. (2017; 3FHL). The purple arrows indicate upper limits at the 95% confidence level derived from the analysis of MAGIC data (∼125 hr) presented in this paper. The green and orange lines show the gamma-ray spectra predicted by the AGN jet (Lenain et al. 2010) and starburst ($p = 2.5$, $E_{\rm cut} = 10^8$ GeV, and $\xi = 0.04$, Eichmann & Becker Tjus 2016) models, respectively. The shaded gray band indicates the upper ($p = 2$, $E_{\rm cut} = 6 \times 10^6$ GeV, and $\xi = 0.25$) and lower ($p = 2$, $E_{\rm cut} = 3 \times 10^5$ GeV, and $\xi = 0.2$) bounds of the gamma-ray emission predicted by the AGN wind model as proposed by Lamastra et al. (2016). For the sake of clarity, the predictions of the revised AGN wind model (Lamastra et al. 2019) are not shown, as they do not differ from that by Lamastra et al. (2016) at energies smaller than 10 TeV. For comparison, the spectrum predicted by the AGN wind model that is obtained by assuming one of the combinations of CR proton spectral parameters compatible with the MAGIC upper limits ($p = 2$, $E_{\rm cut} = 8 \times 10^3$ GeV, and $\xi = 0.2$, see Figure 3), is shown with the dark gray line.

**Table 1**
Spectral Energy Distribution in the VHE Band

| log $E$ (GeV) | $\nu F_\nu$ (erg cm$^{-2}$ s$^{-1}$) |
|---|---|
| 2.25 | $<1.1 \times 10^{-12}$ |
| 2.75 | $<2.8 \times 10^{-13}$ |
| 3.25 | $<1.1 \times 10^{-13}$ |
| 3.75 | $<2.9 \times 10^{-13}$ |

energies only upper limits on the energy flux are determined. At energies ∼10 GeV, an indication of a bump can be seen in the *Fermi*-LAT spectrum. This apparent spectral feature could be ascribed to the energy binning. As discussed in Lamastra et al. (2016), assuming a single bin in the (10–100) GeV energy range, a constant spectrum, like the one reported in the 3FGL *Fermi* catalog (Acero et al. 2015), is obtained above 1 GeV.

In Figure 2, we also show the spectra predicted by the starburst, AGN jet, and AGN wind models that have been proposed to explain the gamma-ray emission (Lenain et al. 2010; Eichmann & Becker Tjus 2016; Lamastra et al. 2016).

Comparison between the predicted and observed gamma-ray spectra indicates that the AGN jet model is in agreement with the observed gamma-ray flux and upper limits. In this model a maximum Lorentz factor of jet leptons of $\gamma_{\rm max} = 10^6$ is assumed in order to produce the sharp cutoff at ∼100 GeV. In contrast, the AGN wind model predicts a hard spectrum extending to the VHE band that is strongly constrained by the MAGIC observations presented in this paper. Finally, the starburst model by Eichmann & Becker Tjus (2016), where the gamma-ray emission is produced within the inner ∼180 pc of the galaxy, is compatible with the VHE limits but cannot describe the *Fermi*-LAT spectrum; the gamma-ray flux at 1 GeV is higher than the model by about a factor of two.

The constrained part of the spectrum predicted by the AGN wind model is the hadronic component that originates from the decay of neutral pions produced in inelastic collisions between protons accelerated by the AGN-driven outflow observed in the molecular disk on a ∼100 pc scale and ambient protons. The leptonic gamma-ray emission predicted by the AGN wind model, as well as that predicted by the AGN jet model, do not extend at TeV energies, owing to the effect of the transition of IC cooling from the Thomson regime to the Klein–Nishina regime. Thus, the limits on the VHE emission can be used to effectively constrain only the hadronic gamma-ray emission of the AGN wind and starburst models.

To derive constraints on the CR proton population of stellar and AGN origin, we compare the gamma-ray spectra predicted by the starburst and AGN wind models with the spectrum measured in the HE band and with the upper limits derived in the VHE band. In both the starburst and AGN wind models, protons are assumed to be accelerated by diffusive shocks with an energy distribution $N(E) = AE^{-p}\ \exp(-E/E_{\rm cut})$, where the normalization constant $A$ is determined by the total energy supplied to relativistic protons at the shock, $p \simeq 2$ is the spectral index, and $E_{\rm cut}$ is the maximum energy of accelerated protons. The latter has a physical maximum limit determined by the Hillas criterion: $E_{\rm max} = 10^{18} Z(R/{\rm kpc})(B/\mu{\rm G}){\rm eV}$, where $Z$ is the atomic charge number, $R$ is the physical extent of the acceleration region, and $B$ is the magnetic field (Hillas 1985), while the minimum energy of accelerated protons is the proton rest mass.

With regard to the the energy input from star formation, because *Fermi*-LAT does not spatially resolve the gamma-ray-emitting region, we consider the total star formation of the galaxy. The kinetic input from star formation is calculated as $L_{\rm kin}^{\rm SF} = \nu_{\rm SN} E_{\rm SN}$, where $\nu_{\rm SN}$ is the supernovae rate, and $E_{\rm SN} \simeq 10^{51}$ erg is the typical kinetic energy from a supernova explosion. We estimated $\nu_{\rm SN} = 0.43\,{\rm yr}^{-1}$ from the total infrared luminosity of the galaxy $L_{\rm IR} \simeq 10^{45}\,{\rm erg\,s}^{-1}$ (between

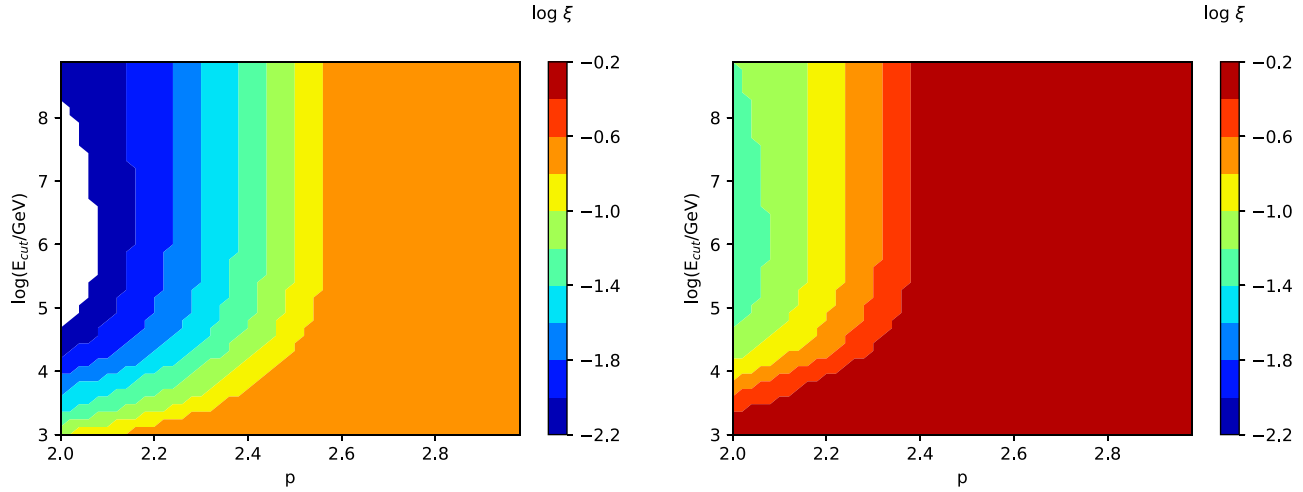


**Figure 3.** The allowed values of the starburst (left) and AGN wind (right) hadronic spectral index $p$ and cutoff energy $E_{\rm cut}$ derived from HE and VHE observations of NGC 1068 are plotted as a function of the product between the calorimetric fraction and the acceleration efficiency $\xi$. The logarithmic values of $\xi$ corresponding to the colored contours are displayed on the vertical bar.

8 and 1000 $\mu$m, Ackermann et al. 2012), and assuming a Kroupa initial mass function (Kroupa 2001; Kennicutt & Evans 2012), yielding $L_{\rm kin}^{\rm SF} = 1.4 \times 10^{43}$ erg s$^{-1}$. We find that the kinetic luminosity provided by the star formation throughout the galaxy can produce the gamma-ray emission measured in the *Fermi*-LAT band.

For the AGN wind model, we derived the kinetic luminosity provided by the AGN from the kinetic luminosity of the molecular outflow, which is observed by millimeter interferometers on a $\sim$100 pc scale, yielding $L_{\rm kin}^{\rm AGN} = (0.5\text{–}1.5) \times 10^{42}$ erg s$^{-1}$ (Krips et al. 2011; García-Burillo et al. 2014; Lamastra et al. 2016). This molecular outflow is likely produced by the interaction of the molecular gas with the AGN jet, and/or the energy released during accretion of matter onto the supermassive black hole, rather than star formation.[49]

The fraction of CR energy input provided by star formation and AGN activity that is emitted in gamma-rays depends on the proton acceleration efficiency, $\eta$, and on the efficiency of converting proton kinetic energy into gamma-rays, $F_{\rm cal}$. The comparison between the gamma-ray emission in star-forming galaxies and the kinetic energy supplied by SN explosions leads to $\eta \simeq (0.1\text{–}0.3)$ and $F_{\rm cal} \simeq 0.3\text{–}0.6$ (Keshet et al. 2003; Tatischeff 2008; Lacki et al. 2010; Ackermann et al. 2012; Wang & Fields 2018).

We compute the gamma-ray spectrum produced by neutral pion decays following proton–proton interactions as in Lamastra et al. (2016; see also Kelner et al. 2006), and varying the CR proton parameters: $p$, $E_{\rm cut}$, and $\xi = \eta \times F_{\rm cal}$. Comparison between the predicted spectra and the upper limits in the VHE band allowed us to derive reliable constraints on these parameters. The results are shown in Figure 3, where for each value of $\xi$, the allowed value of $E_{\rm cut}$ is plotted as a function of $p$ in the starburst and AGN models, separately. In each model we find that, for a given value of $\xi$, the cutoff energy increases with the spectral index up to a value at which $E_{\rm cut}$ becomes independent of the value of $p$. This is determined by the gradually lower influence of the high-energy cutoff on the shape and normalization of the gamma-ray spectrum, depending on the fraction $\xi$ and slope $p$.

The constraints obtained for the CR proton parameters are mainly determined by the MAGIC upper limits in the 0.3–1 and 1–3 TeV energy bins. Gamma-rays with energy above the threshold for electron–positron pair production may be absorbed due to interactions with the extragalactic background light (EBL, e.g., Domínguez et al. 2011; Franceschini & Rodighiero 2017; Acciari et al. 2019), and radiation fields within the galaxy. Both processes contribute in turn to the uncertainty in the computation of $p$ and $E_{\rm cut}$. As discussed in Lamastra et al. (2019), absorption due to the EBL and to the infrared emission from the starburst ring surrounding the acceleration regions affects the gamma-ray spectrum only above $E \gtrsim 10$ TeV, thus the constraints shown in Figure 3 can be considered robust.

## 4. Discussion

The derived properties of the gamma-ray spectrum of NGC 1068 are now compared with the gamma-ray properties of the two starburst galaxies detected in the VHE band. NGC 253 and M82 were detected by H.E.S.S. and VERITAS in $\simeq$180 hr and $\simeq$140 hr of observations, respectively. After the detection at TeV energies, these starburst galaxies were also detected by *Fermi*-LAT. Although the statistic is limited, there is no indication of a spectral break or cutoff features apparent in the spectra. The smooth alignment of the GeV and TeV spectrum suggests that a single energy-loss mechanism dominates in the gamma-ray band. The loss mechanism is probably related to CR proton interactions with ISM. In fact, models assuming that a population of protons is giving rise to the measured gamma-ray spectra through hadronic collisions provide a good fit to the data (Abramowski et al. 2012). Moreover, the lack of variability at any gamma-ray energy supports the idea that the emission is related to star formation processes rather than nuclear activity.

The gamma-ray properties of NGC 1068, including the shape of the gamma-ray spectrum in the HE band and the lack of variability of the *Fermi*-LAT and MAGIC light curves, suggest that the radiation processes are similar to those in other starburst galaxies. However, the extrapolation of the gamma-ray emission

[49] The star formation rate, SFR $\simeq 1\ M_{\odot}$ yr$^{-1}$, for the circumnuclear region up to a radius $R \simeq 140$ pc (Esquej et al. 2014), is unable to power the molecular outflow.

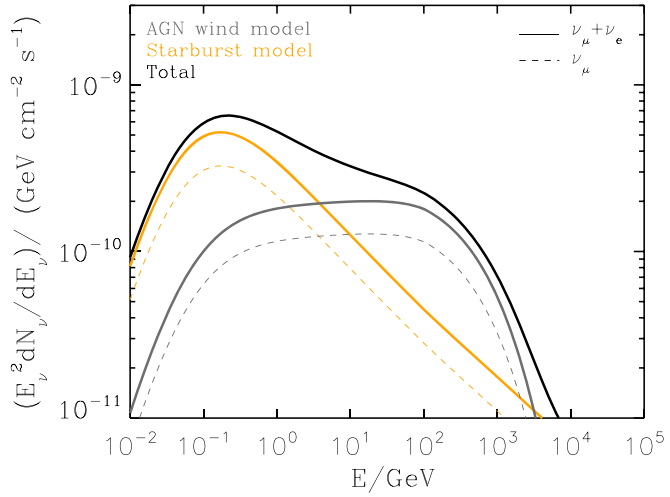


**Figure 4.** Neutrino spectra of NGC 1068 expected in the starburst (orange lines) and AGN wind (gray lines) models. The dashed lines indicate the muon neutrino fluxes, while solid lines indicate the total neutrino fluxes. The solid black line represents the cumulative neutrino spectrum.

of NGC 1068 in the VHE band assuming a single power law with spectral index $p \simeq 2.2$, as resulting from the combined fit of the latest *Fermi*-LAT and H.E.S.S. spectrum of NGC 253 (Abdalla et al. 2018), results in an overprediction of the emission at TeV energies. As shown in Figure 3, in the starburst model a gamma-ray spectrum that extends to energies $E_{\rm cut} \gtrsim 10^4$ GeV with $p = 2.2$ can only be obtained for low calorimetric and acceleration efficiencies ($\xi \lesssim 0.02$,) that produce a gamma-ray flux at 1 GeV lower by about a factor of 10 than that measured by *Fermi*-LAT. In case the emission in the *Fermi*-LAT band is ascribed to star formation, loss mechanisms that make the starburst spectrum soft and/or the proton maximum energy low must operate in the starburst region.

The precise measurements of the gamma-ray spectral properties of starburst galaxies, including those with AGNs, are crucial to determine their contribution to the extragalactic gamma-ray and neutrino backgrounds. The estimates of the source population contribution to the observed backgrounds rely on the extrapolation of the characteristic source spectrum to the region between the HE band and the IceCube energy scale. Analyses that have utilized GeV–TeV gamma-ray spectral information to constrain the contribution of starburst galaxies to the diffuse fluxes measured by *Fermi*-LAT and IceCube found that a characteristic CR proton spectral index of $p \simeq 2.2$ and cutoff energy $E_{\rm cut} = 10^7$ GeV are consistent with the bounds from the residual non-blazar component of the extragalactic gamma-ray background. This yields a contribution to the diffuse neutrino background of 30% at 100 TeV, and 60% at 1 PeV (Bechtol et al. 2017). A harder ($p \simeq 2.1$) spectrum saturates the IceCube signal, while a softer ($p \simeq 2.3$) spectrum underestimates the diffuse neutrino energy flux by about an order of magnitude, remaining compatible with the gamma-ray bounds (Bechtol et al. 2017; Linden 2017; Palladino et al. 2019).

We apply this multi-messenger approach to NGC 1068 and we derive the expected neutrino flux based on the observed gamma-ray flux. In Figure 4 we show the neutrino spectra predicted by the starburst model and by the AGN wind model with CR parameters compatible with VHE upper limits that are shown in Figure 2. To calculate the neutrino spectra we use the parameterizations for the high-energy spectra of secondary particles produced in proton–proton collisions derived by Kelner et al. (2006). We calculate the spectra of muon and electron (anti)neutrinos from muon decays, and the spectra of muon (anti)neutrinos produced through the direct decays of charged pions.

In order to assess the capability of current neutrino detectors in testing the hadronuclear models, following Lamastra et al. (2016), we combine the total neutrino spectra with the effective area of IceCube (Aartsen et al. 2014). We obtain a neutrino event rate with energy $E_\nu > 0.1$ TeV of $0.002\,{\rm yr}^{-1}$ and $0.001\,{\rm yr}^{-1}$ for the starburst and the AGN wind models, respectively. Additionally, we compute the maximum IceCube neutrino event rates, compatible with the MAGIC upper limits, scanning the parameter space of the starburst and AGN wind models, described in Figure 3. We obtain a maximum event rate of $0.07\,{\rm yr}^{-1}$.

The level of neutrino signal predicted by hadronuclear models makes the detection of NGC 1068 a challenge for the current neutrino detectors. A neutrino flux larger than those derived in this paper can be achieved if the source of neutrinos resides in an extremely dense environment that prevents the escape of GeV–TeV gamma-rays. This would mean gamma-ray production occurs in the AGN core, where the intense optical and near-infrared emission produced by the active nucleus and the surrounding dusty torus (Hönig et al. 2008) could act as the target photon field for both photohadronic gamma-ray and neutrino emissions and for pair production (e.g., Murase et al. 2016; Inoue et al. 2019).

## 5. Conclusions

The results from the MAGIC observations of NGC 1068 imply that the gamma-ray spectrum could be either entirely produced by leptonic processes, as in the AGN jet model, or, if a hadronuclear component is present, as envisaged in the AGN wind or in the starburst models, the accelerated proton population should have soft spectra ($p \gtrsim 2.2$) and/or low maximum energy ($E_{\rm cut} \simeq 10^4$ GeV).

At present, it is not possible to spatially resolve the emission from the different components (jet, starburst, molecular disk) in the gamma-ray band with *Fermi*-LAT, thus no strong conclusions can be drawn on their relative contributions to the observed emission. This obstacle could be overcome in principle with observations in the radio band that can potentially benefit also from spatial information. However, the presence of the radio jet in the inner 100 pc hampers the identification of any emission not originating from the jet or the compact nucleus. Firm conclusions cannot be drawn regarding the different contributions on the basis of the non-variability of the gamma-ray flux. In fact, the gamma-ray emission in the AGN jet model may be produced from a few tenths of parsecs up to a hundred parsec from the nucleus (Lenain et al. 2010), and no significant variability is expected for the more distant emitting zone, as in the starburst and AGN wind models.

Improving our understanding of the gamma-ray spectral properties of star-forming galaxies and AGNs is crucial to test source population models of the extragalactic gamma-ray and neutrino backgrounds. Indeed, although coincident observations of neutrinos and gamma-rays from the blazar TXS 0506+056 represent compelling evidence of the first extragalactic neutrino source (Aartsen et al. 2018; Ansoldi et al. 2018), independent analyses indicate that blazars can account only for $\lesssim$30% of the

diffuse neutrino flux measured by IceCube (Murase & Waxman 2016; Padovani et al. 2016; Aartsen et al. 2017).

The astrophysical high-energy neutrino flux observed with IceCube is consistent with an isotropic distribution of neutrino arrival directions, suggesting an extragalactic origin. Star-forming galaxies such as NGC 1068, could be the main contributors to the observed neutrino emission. The increase of the sensitivity up to a factor ∼10, as envisaged in the the next generation of neutrino detectors (such as Km3Net and IceCube-Gen2), will allow the detection of neutrinos from the starburst and AGN wind scenarios described here. The detection of a neutrino signal from these sources would be compelling evidence for the presence of a hadronic component in the gamma-ray spectrum. At the same time, the improved sensitivity of the next generation of ground-based gamma-ray observatories, like the Cherenkov Telescope Array, will allow us to disentangle the different emission mechanisms. In particular, simulations of 50 hr of observations of NGC 1068 with CTA have shown that leptonic and hadronic models could be distinguished (Lamastra et al. 2019).

We would like to thank the referee for useful comments and the Instituto de Astrofísica de Canarias for the excellent working conditions at the Observatorio del Roque de los Muchachos in La Palma. The financial support of the German BMBF and MPG, the Italian INFN and INAF, the Swiss National Fund SNF, the ERDF under the Spanish MINECO (FPA2015-69818-P, FPA2012-36668, FPA2015-68378-P, FPA2015-69210-C6-2-R, FPA2015-69210-C6-4-R, FPA2015-69210-C6-6-R, AYA2015-71042-P, AYA2016-76012-C3-1-P, ESP2015-71662-C2-2-P, FPA201790566REDC), the Indian Department of Atomic Energy, the Japanese JSPS and MEXT, the Bulgarian Ministry of Education and Science, National RI Roadmap Project DO1-153/28.08.2018, and the Academy of Finland grant No. 320045 is gratefully acknowledged. This work was also supported by the Spanish Centro de Excelencia "Severo Ochoa" SEV-2016-0588 and SEV-2015-0548, and Unidad de Excelencia "María de Maeztu" MDM-2014-0369, by the Croatian Science Foundation (HrZZ) Project IP-2016-06-9782 and the University of Rijeka Project 13.12.1.3.02, by the DFG Collaborative Research Centers SFB823/C4 and SFB876/C3, the Polish National Research Centre grant UMO-2016/22/M/ST9/00382, and by the Brazilian MCTIC, CNPq, and FAPERJ.

## ORCID iDs

V. A. Acciari https://orcid.org/0000-0001-8307-2007
S. Ansoldi https://orcid.org/0000-0002-5613-7693
L. A. Antonelli https://orcid.org/0000-0002-5037-9034
A. Babić https://orcid.org/0000-0002-1444-5604
B. Banerjee https://orcid.org/0000-0002-8008-2485
U. Barres de Almeida https://orcid.org/0000-0001-7909-588X
J. A. Barrio https://orcid.org/0000-0002-0965-0259
J. Becerra González https://orcid.org/0000-0002-6729-9022
W. Bednarek https://orcid.org/0000-0003-0605-108X
E. Bernardini https://orcid.org/0000-0003-3108-1141
A. Berti https://orcid.org/0000-0003-0396-4190
W. Bhattacharyya https://orcid.org/0000-0003-4751-0414
C. Bigongiari https://orcid.org/0000-0003-3293-8522
A. Biland https://orcid.org/0000-0002-1288-833X
O. Blanch https://orcid.org/0000-0002-8380-1633
G. Bonnoli https://orcid.org/0000-0003-2464-9077
Ž. Bošnjak https://orcid.org/0000-0002-6551-4913
G. Busetto https://orcid.org/0000-0002-2687-6380
R. Carosi https://orcid.org/0000-0002-4137-4370
Y. Chai https://orcid.org/0000-0003-2816-2821
A. Chilingaryan https://orcid.org/0000-0002-2018-9715
S. M. Colak https://orcid.org/0000-0001-7793-3106
E. Colombo https://orcid.org/0000-0002-3700-3745
J. L. Contreras https://orcid.org/0000-0001-7282-2394
J. Cortina https://orcid.org/0000-0003-4576-0452
S. Covino https://orcid.org/0000-0001-9078-5507
V. D'Elia https://orcid.org/0000-0002-7320-5862
F. Dazzi https://orcid.org/0000-0001-5409-6544
A. De Angelis https://orcid.org/0000-0002-3288-2517
B. De Lotto https://orcid.org/0000-0003-3624-4480
M. Delfino https://orcid.org/0000-0002-9468-4751
J. Delgado https://orcid.org/0000-0002-0166-5464
D. Depaoli https://orcid.org/0000-0002-2672-4141
F. Di Pierro https://orcid.org/0000-0003-4861-432X
L. Di Venere https://orcid.org/0000-0003-0703-824X
E. Do Souto Espiñeira https://orcid.org/0000-0001-6974-2676
D. Dominis Prester https://orcid.org/0000-0002-9880-5039
M. Doro https://orcid.org/0000-0001-9104-3214
D. Elsaesser https://orcid.org/0000-0001-6796-3205
V. Fallah Ramazani https://orcid.org/0000-0001-8991-7744
G. Ferrara https://orcid.org/0000-0002-1137-6252
D. Fidalgo https://orcid.org/0000-0002-7480-2730
L. Foffano https://orcid.org/0000-0002-0709-9707
M. V. Fonseca https://orcid.org/0000-0003-2235-0725
L. Font https://orcid.org/0000-0003-2109-5961
C. Fruck https://orcid.org/0000-0001-5880-7518
R. J. García López https://orcid.org/0000-0002-8204-6832
M. Garczarczyk https://orcid.org/0000-0002-0445-4566
M. Gaug https://orcid.org/0000-0001-8442-7877
N. Giglietto https://orcid.org/0000-0002-9021-2888
F. Giordano https://orcid.org/0000-0002-8651-2394
N. Godinović https://orcid.org/0000-0002-4674-9450
D. Green https://orcid.org/0000-0003-0768-2203
D. Guberman https://orcid.org/0000-0002-9636-1825
D. Hadasch https://orcid.org/0000-0001-8663-6461
A. Hahn https://orcid.org/0000-0003-0827-5642
J. Herrera https://orcid.org/0000-0002-3771-4918
J. Hoang https://orcid.org/0000-0001-5591-5927
D. Hrupec https://orcid.org/0000-0002-7027-5021
M. Hütten https://orcid.org/0000-0002-2133-5251
S. Inoue https://orcid.org/0000-0003-1096-9424
D. Kerszberg https://orcid.org/0000-0002-5289-1509
H. Kubo https://orcid.org/0000-0001-9159-9853
A. Lamastra https://orcid.org/0000-0003-2403-913X
D. Lelas https://orcid.org/0000-0002-8269-5760
F. Leone https://orcid.org/0000-0001-7626-3788
E. Lindfors https://orcid.org/0000-0002-9155-6199
S. Lombardi https://orcid.org/0000-0002-6336-865X
F. Longo https://orcid.org/0000-0003-2501-2270
M. López https://orcid.org/0000-0002-8791-7908
R. López-Coto https://orcid.org/0000-0002-3882-9477
A. López-Oramas https://orcid.org/0000-0003-4603-1884
S. Loporchio https://orcid.org/0000-0003-4457-5431
B. Machado de Oliveira Fraga https://orcid.org/0000-0002-6395-3410

C. Maggio https://orcid.org/0000-0003-0670-7771
P. Majumdar https://orcid.org/0000-0002-5481-5040
M. Makariev https://orcid.org/0000-0002-1622-3116
M. Mallamaci https://orcid.org/0000-0003-4068-0496
G. Maneva https://orcid.org/0000-0002-5959-4179
M. Manganaro https://orcid.org/0000-0003-1530-3031
M. Mariotti https://orcid.org/0000-0003-3297-4128
M. Martínez https://orcid.org/0000-0002-9763-9155
D. Mazin https://orcid.org/0000-0002-2010-4005
S. Mićanović https://orcid.org/0000-0002-0076-3134
D. Miceli https://orcid.org/0000-0002-2686-0098
J. M. Miranda https://orcid.org/0000-0002-1472-9690
E. Molina https://orcid.org/0000-0003-1204-5516
A. Moralejo https://orcid.org/0000-0002-1344-9080
D. Morcuende https://orcid.org/0000-0001-9400-0922
V. Moreno https://orcid.org/0000-0002-8358-2098
E. Moretti https://orcid.org/0000-0001-5477-9097
P. Munar-Adrover https://orcid.org/0000-0002-1942-7376
V. Neustroev https://orcid.org/0000-0003-4772-595X
C. Nigro https://orcid.org/0000-0001-8375-1907
K. Nilsson https://orcid.org/0000-0002-1445-8683
D. Ninci https://orcid.org/0000-0002-5031-1849
K. Nishijima https://orcid.org/0000-0002-1830-4251
K. Noda https://orcid.org/0000-0003-1397-6478
L. Nogués https://orcid.org/0000-0002-6482-1671
S. Paiano https://orcid.org/0000-0002-2239-3373
J. Palacio https://orcid.org/0000-0003-0374-100X
M. Palatiello https://orcid.org/0000-0002-4124-5747
D. Paneque https://orcid.org/0000-0002-2830-0502
R. Paoletti https://orcid.org/0000-0003-0158-2826
J. M. Paredes https://orcid.org/0000-0002-1566-9044
M. Peresano https://orcid.org/0000-0002-7537-7334
M. Persic https://orcid.org/0000-0003-1853-4900
P. G. Prada Moroni https://orcid.org/0000-0001-9712-9916
E. Prandini https://orcid.org/0000-0003-4502-9053
I. Puljak https://orcid.org/0000-0001-7387-3812
W. Rhode https://orcid.org/0000-0003-2636-5000
M. Ribó https://orcid.org/0000-0002-9931-4557
J. Rico https://orcid.org/0000-0003-4137-1134
C. Righi https://orcid.org/0000-0002-1218-9555
A. Rugliancich https://orcid.org/0000-0001-5471-4701
L. Saha https://orcid.org/0000-0002-3171-5039
N. Sahakyan https://orcid.org/0000-0003-2011-2731
K. Satalecka https://orcid.org/0000-0002-7669-266X
K. Schmidt https://orcid.org/0000-0002-9883-4454
J. Sitarek https://orcid.org/0000-0002-1659-5374
D. Sobczynska https://orcid.org/0000-0003-4973-7903
A. Somero https://orcid.org/0000-0001-6566-9192
A. Stamerra https://orcid.org/0000-0002-9430-5264
D. Strom https://orcid.org/0000-0003-2108-3311
Y. Suda https://orcid.org/0000-0002-2692-5891
M. Takahashi https://orcid.org/0000-0002-0574-6018
F. Tavecchio https://orcid.org/0000-0003-0256-0995
P. Temnikov https://orcid.org/0000-0002-9559-3384
T. Terzić https://orcid.org/0000-0002-4209-3407
N. Torres-Albà https://orcid.org/0000-0003-3638-8943
V. Vagelli https://orcid.org/0000-0002-4495-9331
J. van Scherpenberg https://orcid.org/0000-0002-6173-867X
M. Vazquez Acosta https://orcid.org/0000-0002-2409-9792
C. F. Vigorito https://orcid.org/0000-0002-0069-9195
V. Vitale https://orcid.org/0000-0001-8040-7852
I. Vovk https://orcid.org/0000-0003-3444-3830
M. Will https://orcid.org/0000-0002-7504-2083
D. Zarić https://orcid.org/0000-0001-5763-9487
F. Fiore https://orcid.org/0000-0002-4031-4157
C. Feruglio https://orcid.org/0000-0002-4227-6035
Y. Rephaeli https://orcid.org/0000-0002-9947-2897

## References

Aartsen, M. G., Abraham, K., Ackermann, M., et al. 2015, ApJ, 809, 98
Aartsen, M. G., Abraham, K., Ackermann, M., et al. 2017, ApJ, 835, 45
Aartsen, M. G., Ackermann, M., Adams, J., et al. 2014, ApJ, 796, 109
Aartsen, M. G., Ackermann, M., Adams, J., et al. 2018, Sci, 361, eaat1378
Abdalla, H., Aharonian, F., Ait Benkhali, F., et al. 2018, A&A, 617, A73
Abramowski, A., Acero, F., Aharonian, F., et al. 2012, ApJ, 757, 158
Acciari, V. A., Aliu, E., Arlen, T., et al. 2009, Natur, 462, 770
Acciari, V. A., Ansoldi, S., Antonelli, L. A., et al. 2019, MNRAS, 486, 4233
Acero, F., Aharonian, F., Akhperjanian, A. G., et al. 2009, Sci, 326, 1080
Acero, F., Akermann, M., Ajello, M., et al. 2015, ApJS, 218, 23
Ackermann, M., Ajello, M., Albert, A., et al. 2015, ApJ, 799, 86
Ackermann, M., Ajello, M., Allafort, A., et al. 2012, ApJ, 755, 164
Aharonian, F., Akhperjanian, A. G., Bazer-Bachi, A. R., et al. 2005, A&A, 441, 465
Ahnen, M. L., Ansoldi, S., Antonelli, L. A., et al. 2017, APh, 94, 29
Ajello, M., Atwood, W. B., Baldini, L., et al. 2017, ApJS, 232, 18
Aleksić, J., Ansoldi, S., Antonelli, L. A., et al. 2016, APh, 72, 76
Ansoldi, S., Antonelli, L. A., Arcaro, C., et al. 2018, ApJL, 863, L10
Bechtol, K., Ahlers, M., Di Mauro, M., Ajello, M., & Vandenbroucke, J. 2017, ApJ, 836, 47
Domínguez, A., Primack, J. R., Rosario, D. J., et al. 2011, MNRAS, 410, 2556
Eichmann, B., & Becker Tjus, J. 2016, ApJ, 821, 87
Elmouttie, M., Haynes, R. F., Jones, K. L., Sadler, E. M., & Ehle, M. 1998, MNRAS, 297, 1202
Esquej, P., Alonso-Herrero, A., González-Martín, O., et al. 2014, ApJ, 780, 86
Fomin, V. P., Stepanian, A. A., Lamb, R. C., et al. 1994, APh, 2, 137
Franceschini, A., & Rodighiero, G. 2017, A&A, 603, A34
Gallimore, J. F., Baum, S. A., O'Dea, C. P., & Pedlar, A. 1996, ApJ, 458, 136
García-Burillo, S., Combes, F., Usero, A., et al. 2014, A&A, 567, A125
Gatti, M., Lamastra, A., Menci, N., Bongiorno, A., & Fiore, F. 2015, A&A, 576, A32
Hayashida, M., Stawarz, L., Cheung, C. C., et al. 2013, ApJ, 779, 131
Hernquist, L. 1989, Natur, 340, 687
Hillas, A. M. 1985, Proc. ICRC, 3, 445
Hönig, S. F., Prieto, M. A., & Beckert, T. 2008, A&A, 485, 33
Inoue, Y., Khangulyan, D., Inoue, S., & Doi, A. 2019, arXiv:1909.02239
Kelner, S. R., Aharonian, F. A., & Bugayov, V. V. 2006, PhRvD, 74, 034018
Kennicutt, R. C., & Evans, N. J. 2012, ARA&A, 50, 531
Keshet, U., Waxman, E., Loeb, A., Springel, V., & Hernquist, L. 2003, ApJ, 585, 128
Krips, M., Martín, S., Eckart, A., et al. 2011, ApJ, 736, 37
Kroupa, P. 2001, MNRAS, 322, 231
Lacki, B. C., Thompson, T. A., & Quataert, E. 2010, ApJ, 717, 1
Lamastra, A., Fiore, F., Guetta, D., et al. 2016, A&A, 596, A68
Lamastra, A., Menci, N., Fiore, F., & Santini, P. 2013a, A&A, 552, A44
Lamastra, A., Menci, N., Fiore, F., et al. 2013b, A&A, 559, A56
Lamastra, A., Menci, N., Fiore, F., et al. 2017, A&A, 607, A18
Lamastra, A., Tavecchio, F., Romano, P., Landoni, M., & Vercellone, S. 2019, APh, 112, 16
Lenain, J.-P., Ricci, C., Türler, M., Dorner, D., & Walter, R. 2010, A&A, 524, A72
Li, T. P., & Ma, Y. Q. 1983, ApJ, 272, 317
Linden, T. 2017, PhRvD, 96, 083001
Liu, R.-Y., Murase, K., Inoue, S., Ge, C., & Wang, X.-Y. 2018, ApJ, 858, 9
Murase, K., Guetta, D., & Ahlers, M. 2016, PhRvL, 116, 071101
Murase, K., & Waxman, E. 2016, PhRvD, 94, 103006
Murray, N., & Rahman, M. 2010, ApJ, 709, 424
Padovani, P., Resconi, E., Giommi, P., Arsioli, B., & Chang, Y. L. 2016, MNRAS, 457, 3582
Palladino, A., Fedynitch, A., Rasmussen, R. W., & Taylor, A. M. 2019, JCAP, 8, 004
Peng, F.-K., Wang, X.-Y., Liu, R.-Y., Tang, Q.-W., & Wang, J.-F. 2016, ApJL, 821, L20
Persic, M., Rephaeli, Y., & Arieli, Y. 2008, A&A, 486, 143

Rephaeli, Y., Arieli, Y., & Persic, M. 2010, MNRAS, 401, 473
Rodighiero, G., Brusa, M., Daddi, E., et al. 2015, ApJL, 800, L10
Rolke, W. A., López, A. M., & Conrad, J. 2005, NIMPA, 551, 493
Sanders, D. B., & Mirabel, I. F. 1996, ARA&A, 34, 749
Smith, L. F., Biermann, P., & Mezger, P. G. 1978, A&A, 66, 65
Somerville, R. S., Primack, J. R., & Faber, S. M. 2001, MNRAS, 320, 504
Tamborra, I., Ando, S., & Murase, K. 2014, JCAP, 9, 043
Tang, Q.-W., Wang, X.-Y., & Tam, P.-H. T. 2014, ApJ, 794, 26
Tatischeff, V. 2008, arXiv:0804.1004
The Fermi-LAT Collaboration 2019, arXiv:1902.10045
Wang, X., & Fields, B. D. 2018, MNRAS, 474, 4073
Wang, X., & Loeb, A. 2016, NatPh, 12, 1116
Wojaczyński, R., & Niedźwiecki, A. 2017, ApJ, 849, 97
Yoast-Hull, T. M., Gallagher, J. S., III, Zweibel, E. G., & Everett, J. E. 2014, ApJ, 780, 137
Zschaechner, L. K., Walter, F., Bolatto, A., et al. 2016, ApJ, 832, 142